



Finite-element modelling of reinforced concrete

Master Thesis

CHIRUTA GEORGE

4th SEMESTER, M.Sc. in STRUCTURAL AND CIVIL ENGINEERING

SCHOOL OF ENGINEERING AND SCIENCE

© Aalborg University, spring 2014

George Chiruta.

The content of the report is free for all, but publications (with source) may only occur by an agreement with authors.

This work is printed with LM Roman 12 11pt. Layout and typography is made by the authors with the use of Microsoft Word ™.

4th semester
M. Sc. in Structural and Civil
Engineering

School of Engineering and Science
Telefon 9940 8484
Fax 9940 8552
<http://www.civil.aau.dk/>

Title:

Finite-element modelling of reinforced concrete

Project period:

Spring semester 2015

Supervisors, in alphabetic order:

Johan Clausen

Number of pages:

38

Closed the:

10-06-2015

Synopsis:

In this project a Finite Element analysis is performed on a singly reinforced concrete beam and on a doubly reinforced concrete beam.

Different plasticity models are used for the concrete material in order to test the accuracy of each one of them into the Finite Element method in Abaqus.

Analytical calculations are correspondingly performed in the interest of comparing the numerical analysis with the analytical result.

The moment-rotation curve from Abaqus is compared with the moment capacity calculated in the analytical analysis as well as the stress and strain distribution along the cross section of the beam.

George Chiruță

Signature:

Table of contents

TABLE OF CONTENTS	III
PREFACE	V
1 INTRODUCTION	1
1.1 Reinforced concrete	1
1.2 Project objective	5
1.3 Validation of results	5
2 ANALYTICAL ANALYSIS	6
2.1 Beam proprieties and assumptions	7
2.2 Singly reinforced beam	9
2.3 Doubly reinforced beam	11
2.4 Results	15
3 NUMERICAL ANALYSIS	17
3.1 Material Proprieties	18
3.2 Geometry	22
3.3 Boundary Conditions and Constrains	24
3.4 Mesh system	26
3.5 Results	28
4 COMPARISON	34
4.1 Bending moment	34
4.2 Stresses	35
4.3 Strains	36
5 CONCLUSION	38
BIBLIOGRAPHY	39

Preface

The master thesis is a 4nd semester project in the Master's program in Structural and Civil Engineering and it is written by George Chiruță, student at Aalborg University.

The project deals with the structural analysis of a reinforced concrete beam. It is done with an analytical and a numerical study.

The project is carried out during January to June 2015 and the supervisor of the project is Johan Clausen.

Different programs have been used to perform the needed calculations during the project, these and the chapters where they have been used is explained in the following table:

Software	Purpose
<i>Mathcad</i>	Analytical calculations
<i>Abaqus CAE</i>	FEM Analysis
<i>Archicad 18</i>	Drawings
<i>Excel 2010</i>	Graphs

1 Introduction

1.1 Reinforced concrete

Reinforced concrete is a very common composite material which is formed by combining concrete and reinforcement which has the main goal of compensating for the relatively low tensile strength and ductility of concrete. The reinforcement, which most of the time are steel bars represents all the interconnected bars inside the concrete that strengthen the construction. The consolidation of the two materials behaves very well as there is almost no slippage between the two and more than that the concrete acts like a protective layer for the steel bar exposed to corrosion

The high use of reinforced concrete all over the world is due to the advantages that the material presents (1):

- It has a high strength as concrete resist compression and steel resist tension forces
- It has high fire resistance
- It is a versatile material, can be cast to take a wide variety of shapes and sizes.
- It has low cost of maintenance

However, reinforced concrete, like any other material, does not present only advantages. There are certain characteristics that can lead to the selection of another structural material:

- It requires mixing, casting and curing, processes that can affect the final strength of the structure
- The forms that are required to cast the concrete in place are not economically advantageous
- Shrinkage generates crack development and strength loss

1.1.1 Material Properties

In order to have a good knowledge of how reinforced concrete acts while subjected to external loads, the user needs to possess an adequate understanding of the properties of its components, hence a brief introduction to concrete and steel reinforcement is being presented below.

As concrete is made from cement, aggregate and water it is likewise a composite material. The components are mixed together in proper proportion that can vary slightly, adjusting the properties of the model so it can fit a certain purpose. Following, the concrete increases in strength, reaching its characteristic strength after 28 days (2). As mentioned above tensile stresses are very small and as a result, compressive strength, f_c , is the main criteria of determining the quality of concrete

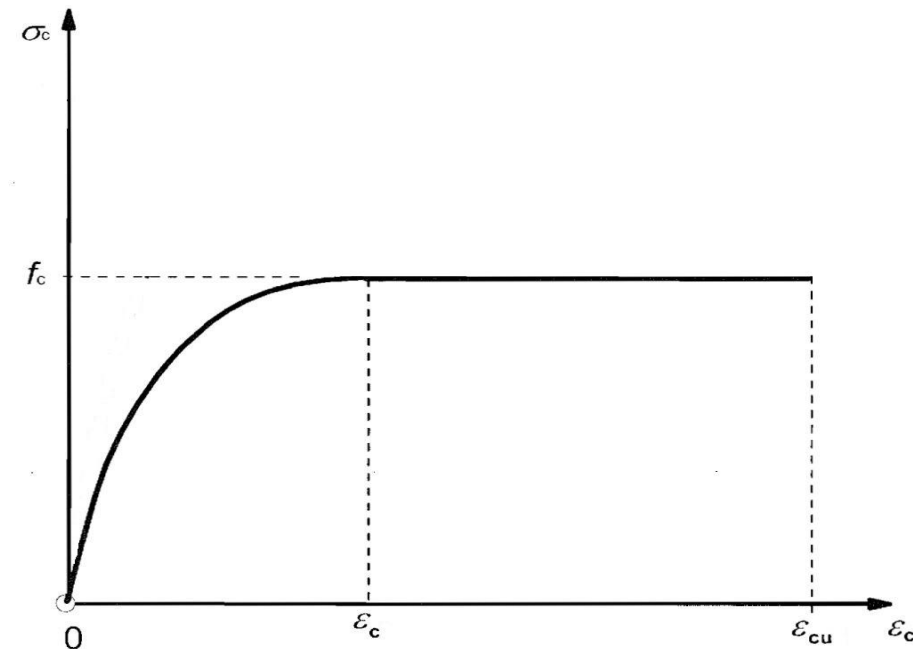


Figure 1.1.1 Stress-strain relations for design of cross-sections (2)

The simplified elastic perfectly-plastic stress-strain curve presented in Figure 1.1.1 is assumed for compressive strength of concrete material. This graph representing the relation between compressive stresses and strains is essential in understanding the behaviour of concrete. It can be observed that from zero to about one half of the maximum stress level the curve is roughly linear (3), beyond that point the behaviour of concrete is nonlinear, this significant aspect causes difficulties regarding the structural analysis of the material.

Reinforcement, typically steel bars are a ductile high strength material that have a ribbed surface to produce an improved bond with concrete. Unlike concrete, steel is a homogenous material that is taken to behave the same in tension as in compression. The idealised stress strain curve elastic perfectly plastic is presented in Figure 1.1.2 where the elastic behaviour is well delimited and it lasts until the yielding strength, f_y , is reached and after the material behaves plastic, deformations being irreversible.

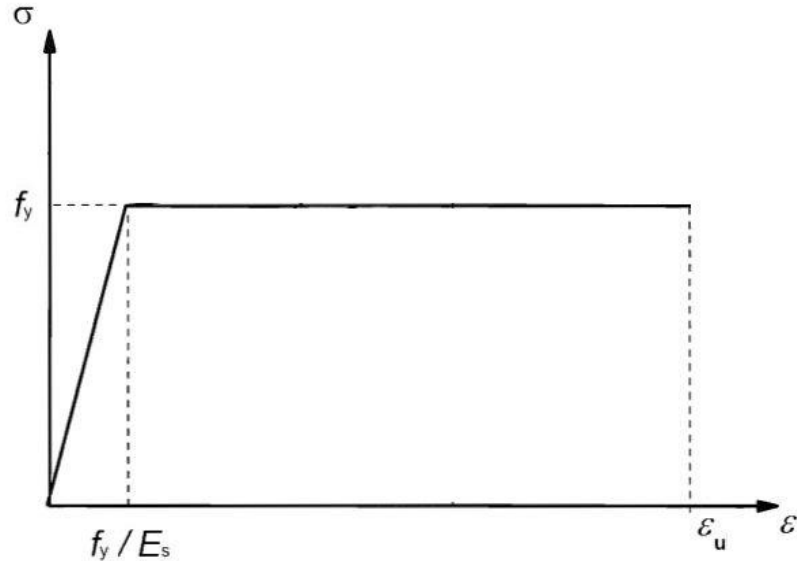


Figure 1.1.2 Idealised stress-Strain curve for reinforcing bars

Even if the main reason is to compensate for the weak tensile strength of concrete, reinforcement are likewise used to reinforce the compression area when heavy loads are acting on the structure (4). In beams there are also reinforcements transverse to the path of main steel and bent in a rectangle shape to prevent shear failure, called stirrups

1.1.2 Beam geometry and cross section

For this master thesis a singly reinforced concrete (RC) beam and a doubly RC beam simply supported and subjected to pure bending are selected for comparison between analytical and numerical methods. The two beam geometries and cross-sections are presented in Figure 1.1.3 and Figure 1.1.4.

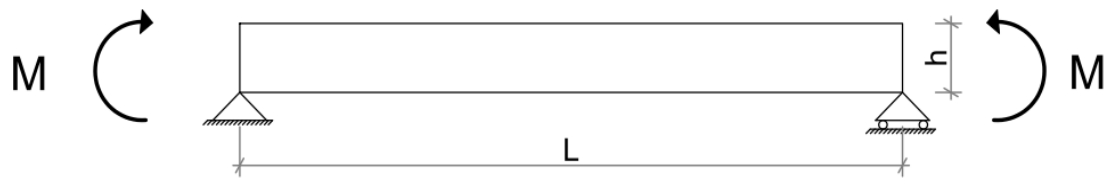
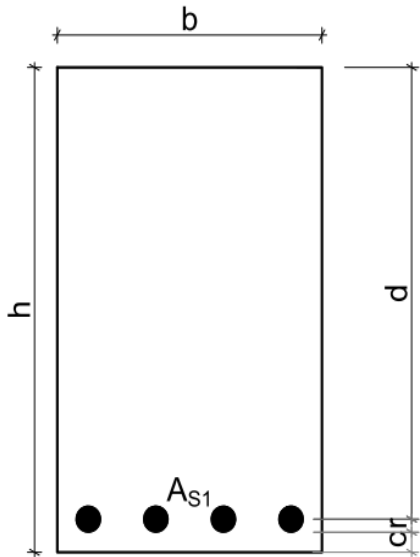


Figure 1.1.3 Beam geometry

Singly RC Beam



Doubly RC Beam

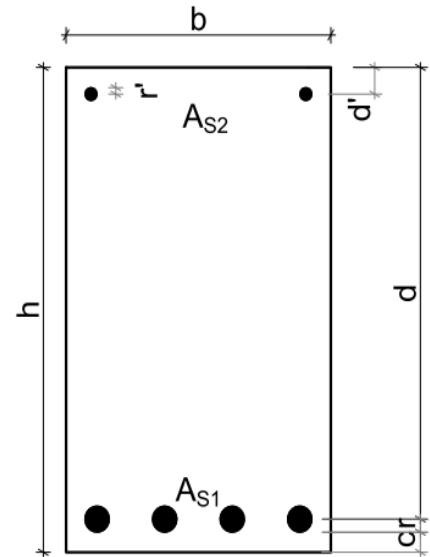


Figure 1.1.4 Cross sections

Length L	6000 mm
Width b	350 mm
Height h	600 mm
Effective depth d	559 mm
Depth of compression steel d'	33 mm
Concrete cover c	25 mm
Radius of reinforcement in tension r	16 mm
Radius of reinforcement in compression r'	8 mm
Area of steel in tension A_{s1}	3216.9 mm ²
Area of steel in compression A_{s2}	402.12 mm ²

Table 1.1.1 Beam properties

1.2 Project objective

The goal of this project is to use finite element calculation to model two types of reinforced concrete beams; one singly reinforced having only tension reinforcement and one doubly reinforced with reinforcement in tension and also in compression. Further, to implement plasticity models that are compatible with concrete material into the finite element method with the intention of obtaining the moment capacity and the stress and strain distribution. A classical analytical method is also carried out.

As a final point a comparison between the numerical analysis and the analytical calculations is done in order to detect the accuracy of the plasticity methods available in Abaqus and to determine which plastic method is more suitable for determining the strength parameters of concrete.

1.3 Validation of results

As a method of validating the analyses that are performed in this project, a test study is executed on a simple beam with the same dimensions and static system as the one in Figure 1.1.3 but on a homogenous material without reinforcements.

From the numerical analysis in Abaqus the moment-rotation curve is compared with the simple analytical calculations for the maximum moment and also with respect to the angle of rotation taken from Abaqus the elastic moment is found and plotted to see if it fits with the moment rotation curve in the elastic part.

The results of the test study, displayed in Appendix A, are confirming that the approach used in this master thesis for modelling the beam is giving precise result and it is concluded that it can be used further for the reinforced concrete beam.

2 Analytical Analysis

In this chapter the two reinforced beam models, with and without compression reinforcement, are being examined analytically regarding bending moment capacity, stress diagram and strains diagrams and compared in the 4th Chapter with the results from the numerical analysis.

This part is build up by introducing all the geometrical and strength parameters needed for the analysis, afterward the assumption that need to be considered in order to perform the analytical calculation are presented. Eventually the steps of the analysis leading to the desired results are revealed.

The calculations from the analytical part are performed in Mathcad software and the drawings are executed in Archicad. All the calculations needed for this analysis are included in the Appendix CD and in Appendix B.

2.1 Beam properties and assumptions

The beam geometry and the materials strength and stiffness parameters are presented in Table 2.1.1. They are chosen arbitrarily, however all the properties of the beam are selected by taking into account the Eurocode requirements and limitations. Area of steel is chosen so that the beam is normally reinforced which means that the steel is yielding alongside with the concrete and the failure is ductile.

Length	6000 mm
Width	350 mm
Height	600 mm
Concrete strength	30 $\frac{N}{mm^2}$
Concrete ultimate strain	0.0035
Concrete cover	25 mm
Steel strength	460 $\frac{N}{mm^2}$
Modulus of elasticity of steel	$2 \times 10^5 \frac{N}{mm^2}$
Yield strain of concrete	0.002
Radius of reinforcement in tension	16 mm
Area of steel in tension	3216.9 mm^2
Radius of reinforcement in compression	8 mm
Area of steel in compression	402.12 mm^2

Table 2.1.1 Beam properties

Since reinforced concrete structures are formed of two materials, they are not homogeneous so conventional plastic methods are not giving convincing results. However, plasticity theory offers a more complex approach in order to find the ultimate strength of a RC section. According to the European Standard (2) the following assumptions are necessary for this analysis:

- Bernoulli's hypothesis holds true, this states that plane section before bending remains plane and perpendicular to the neutral axis after bending.
- Strain is assumed to be linear as is directly proportional to the length from the neutral axis.
- Strain in steel has the same value as the surrounding concrete; this is valid in both tension and compression.
- Tensile strength of concrete is neglected. In reality concrete has a tensile strength of about 10% of the compressive strength; however this assumption is established from the fact that in its ultimate state the tensile part of concrete presents cracks

therefore the tensile strength does not have a significant contribution to the effective part (1).

- The strain at the moment of failure in concrete is assumed to be 0.0035 according to the Eurocode.
- To simplify the calculations the shape of the compressive strength stress distribution is assumed to be rectangular.
- The beam is assumed to be weightless.

The static system of the beam models is shown in the Figure 2.1.1. It is seen that the moment is constant along the length of the beam hence the beam is subjected to pure bending so no axial, shear or torsional forces are presented. This leads as to the fact that the interest is on finding the load-carrying capacity in bending.

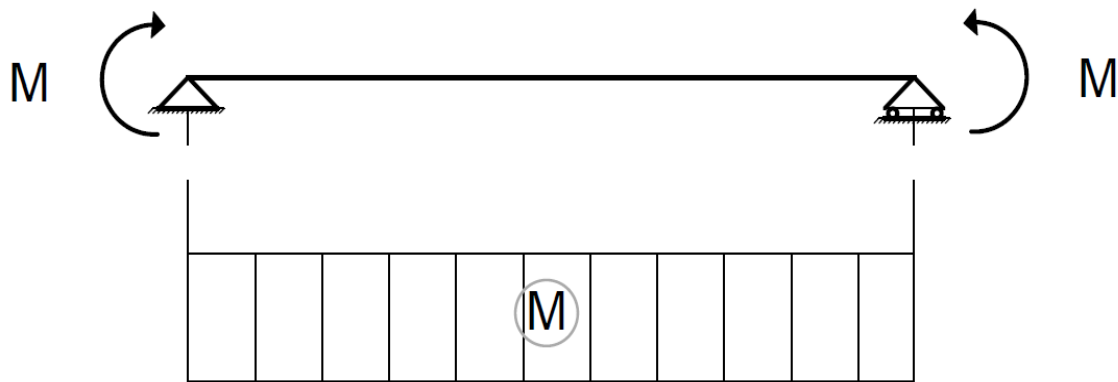


Figure 2.1.1 Static system of the beam

2.2 Singly reinforced beam

The analysis is carried out for the normally reinforced beam with tension reinforcement only. Alongside with the section of the beam, the distribution of the strains and stresses are plotted with respect to the assumption mentioned in subchapter 2.1. The distribution of strains goes from $\varepsilon_{cu}=0.0035$ to the value of 0 when intersecting the neutral axis, then increases proportional with the distance from the neutral axis until reaches the steel strain ε_s . Taking in consideration that the load carrying capacity is wanted and the beam is normally reinforced, $\varepsilon_s > \varepsilon_y$ is necessary to be true, ε_y being the yield strain of steel. Proceeding to the stress distribution where the Eurocode (2) suggests a rectangular stress block to be used in detriment of the real shape of a parabola, for the reason that experiments have proven that this simplified approach is done without a deficit in accuracy (5). The maximum bending moment is found by using basic mechanics of materials, more exactly principle of equilibrium of internal couples on the beam section shown in Figure 2.2.1.

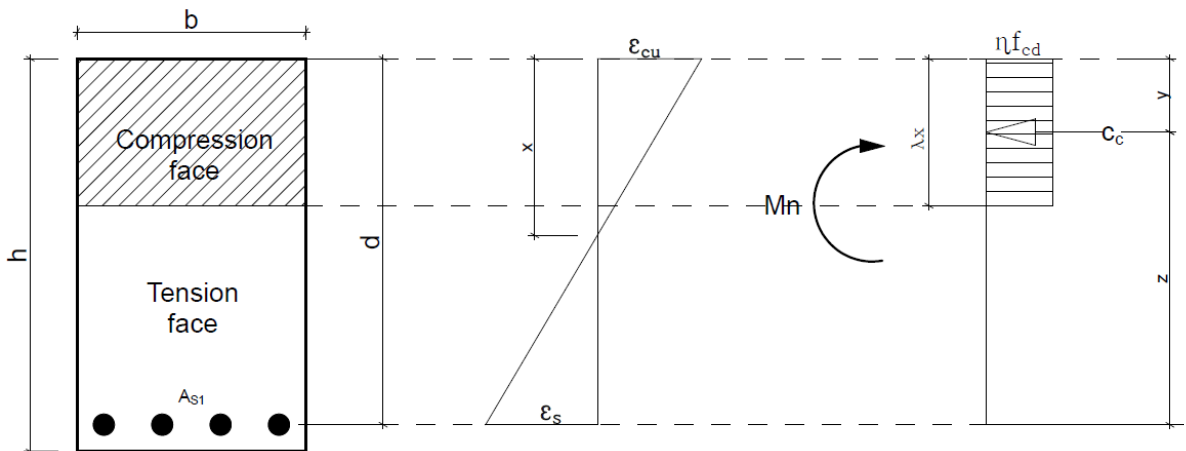


Figure 2.2.1 Singly RC Beam section with strain and stress distributions

The terms in Figure 2.2.1 are defined as follow:

- d Effective height
- h Height of the beam
- b Width of the beam
- A_{s1} Area of all tensile steel bars
- x Depth of the neutral axis
- λ Factor defining the effective height of the compression zone
- z Lever arm of internal forces

- ε_{cu} Ultimate compressive strain in concrete
 ε_s Strain in steel
 η Factor defining the effective strength of concrete
 f_c Compressive strength of concrete
 f_s Tensile strength of steel
 C_c Resultant of the concrete compressive forces
 T_s Resultant of the steel tensile forces
 M_n Maximum moment in bending

Using the strength parameters that are chosen in Table 2.1.1, the values for the factors influencing the strength of concrete are determined as $\lambda = 0.8$ and $\eta = 1$ according to the Eurocode (2). With $\varepsilon_{cu}=0.0035$ known from subchapter 2.1 the analysis can proceed.

Horizontal equilibrium condition:

$$C_c = T_s \quad (2.2.1)$$

With

$$C_c = f_c \times b \times \lambda x \quad (2.2.2)$$

$$T_s = f_s \times A_{s1} \quad (2.2.3)$$

By introducing equations (2.2.2) and (2.2.3) into (2.2.1) and assuming that the steel is yielding which means that $f_s = f_y$ (f_y – the yielding stress of steel), the position of the neutral axis, x , can be determined. Knowing where x is located the value of the steel strain ε_s can be establish by using the similarity of triangles in the strain distribution from Figure 2.2.1. Likewise, the placement of the neutral axis is used to find the length of stress distribution x_c

$$x = \frac{A_{s1} \times f_y}{\lambda \times f_c \times b} \quad (2.2.4)$$

$$\varepsilon_s = \left(\frac{d - x}{x} \right) \varepsilon_{cu} \quad (2.2.5)$$

$$\lambda = 0.8 \quad (2.2.6)$$

- λ Factor defining the effective height of the compression zone

Next step an extra verification to confirm that the steel reinforcements yield before the concrete gets crushed is performed. To verify the yielding of the steel bars, the calculated strain is compared with the yield strain obtained from Hooke's Law.

$$\varepsilon_y = \frac{f_y}{E_s} \quad (2.2.7)$$

After comparison $\varepsilon_s \geq \varepsilon_y$ holds true, and therefore $f_s = f_y$ is true, that means the failure in the beam has a ductile behaviour as recommended by the standards in use, hence before the brittle sudden crush of the concrete, the steel starts yielding and deforming, exhibiting a warning that failure is imminent.

From the equilibrium of moments the value of the maximum bending moment is found:

$$M_n = T_s \times z \quad (2.2.8)$$

Where:

$$z = d - \frac{1}{2} \lambda x \quad (2.2.9)$$

$$T_s = f_s \times A_{s1} \quad (2.2.10)$$

The results are presented in section 2.4

2.3 Doubly reinforced beam

This analysis is concentrated on the beam section with tensile and compression reinforcement and as well as in section 2.2 the goal is to find maximum bending moment and stress and strain distributions. In design, the compression reinforcement is needed often with a nominal value just to provide framework for the shear reinforcement, named stirrups (6), however when the external bending moment is higher than the moment

strength, and the area of steel in tension has reach a maximum amount specified by the standards in use, compression reinforcement must be applied to increase the strength of the beam's section. Also doubly reinforced concrete beams react well to long time deflections, increasing the life of the structure.

The calculations are carried out in the same manner as for the singly reinforced beam and are presented in the following part along with Figure 2.3.1 where the configuration of the beam is presented.

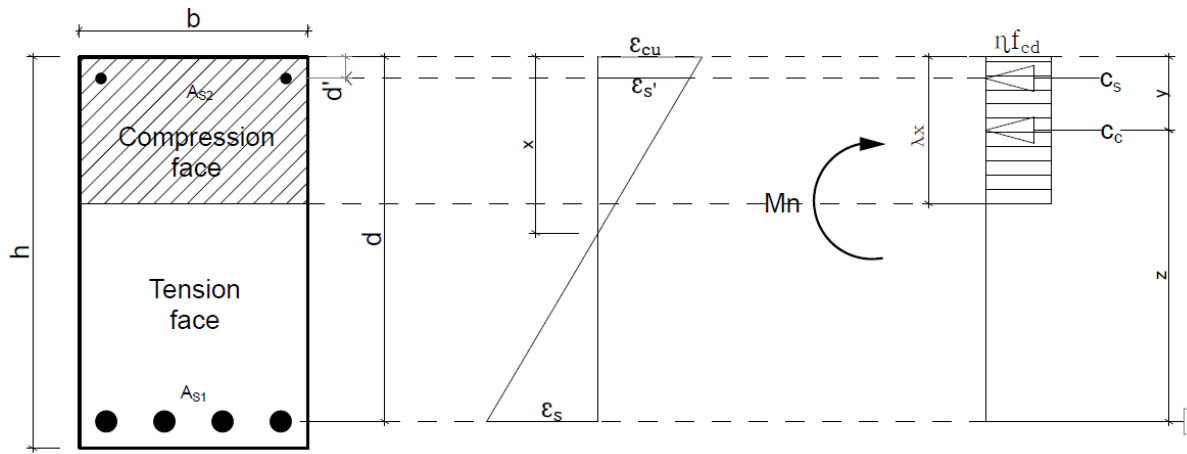


Figure 2.3.1 Doubly RC Beam section with strain and stress distributions

The terms in Figure 2.3.1 are defined as follow

- d Depth to tensile force resultant from the exterior compressive fiber
- d' Depth to compression steel resultant from the exterior compressive fiber
- h Height of the beam
- b Width of the beam
- A_{s1} Area of all tensile steel bars
- A_{s2} Area of all compressive steel bars
- x Depth of the neutral axis
- λ Factor defining the effective height of the compression zone
- z Lever arm of internal forces
- y Depth to the C_c from the exterior compressive fiber
- ε_{cu} Ultimate compressive strain in concrete

ε_s	Strain in steel in tension
ε'_s	Strain in steel in compression
η	Factor defining the effective strength of concrete
f_c	Compressive strength of concrete
f_s	Tensile strength of steel
C_s	Resultant of the steel compressive forces
C_c	Resultant of the concrete compressive forces
T_s	Resultant of the steel tensile forces
M_n	Maximum moment in bending

Horizontal equilibrium condition

$$C_c + C_s = T_s \quad (2.3.1)$$

With

$$C_c = f_c \times b \times \lambda x \quad (2.3.2)$$

$$T_s = f_{s1} \times A_{s1} \quad (2.3.3)$$

$$C_s = f_{s2} \times A_{s2} \quad (2.3.4)$$

By introducing equations (2.3.2), (2.3.3) and (2.3.4) into (2.3.1) and assuming that the steel is yielding in tension which means that $f_{s1} = f_y$ (f_y – the yielding stress of steel) and the stress for steel in compression is found from Hooke's Law, equation (2.3.5) and (2.3.6) are obtained. Determining ε'_s formula from similarity of triangles of strain distribution and introducing it into (2.3.6) and further into (2.3.5) the position of the neutral axis, x , can be determined. The values of the steel strains ε_s and ε'_s can be establish. Likewise, the placement of the neutral axis is used to find the length of stress distribution λx

$$x = \frac{A_{s1} \times f_y - A_{s2} \times f_{s2}}{\lambda \times f_c \times b} \quad (2.3.5)$$

$$f_{s2} = E_s \times \varepsilon'_s \quad (2.3.6)$$

$$\varepsilon_s = \left(\frac{d - x}{x} \right) \varepsilon_{cu} \quad (2.3.7)$$

$$\varepsilon_s' = \left(\frac{x - d'}{x} \right) \varepsilon_{cu} \quad (2.3.8)$$

$$\lambda = 0.8 \quad (2.3.9)$$

λ Factor defining the effective height of the compression zone

In order to validate the calculation a comparison between the yield stress of steel and the actual strains in tension and compression is executed. To verify the yielding of the steel bars, the calculated strain is compared with the yield strain obtained from Hook's Law.

$$\varepsilon_y = \frac{f_y}{E_s} \quad (2.3.10)$$

After comparison $\varepsilon_s \geq \varepsilon_y$ holds true, and therefore $f_s = f_y$.

From the equilibrium of moments the value of the maximum bending moment is found:

$$M_n = C_s \times (y - d') + T_s \times z \quad (2.3.11)$$

Where:

$$z = d - y \quad (2.3.12)$$

$$C_s = f_y \times A_{s2} \quad (2.3.13)$$

$$y = 0.5 \times \lambda x \quad (2.3.14)$$

$$T_s = f_y \times A_{s1} \quad (2.3.15)$$

$$d' = rc + c \quad (2.3.16)$$

r_c Radius of the steel section in compression

c Concrete cover

2.4 Results

The results from both analyses are displayed in the next table:

	Singly RC Beam	Doubly RC Beam
Moment capacity $[N \times mm]$	7.2229×10^8	7.434×10^8
Strain of steel in tension ε_s	0.0076	0.00954
Strain of steel in compression ε_s'	-	0.00273
Length of the neutral axis x [mm]	176.17	150.03
Length of stress distribution λx [mm]	140.94	120.024
Effective depth [mm]	559	559
η	1	1
λ	0.8	0.8

Table 2.4.1 Results

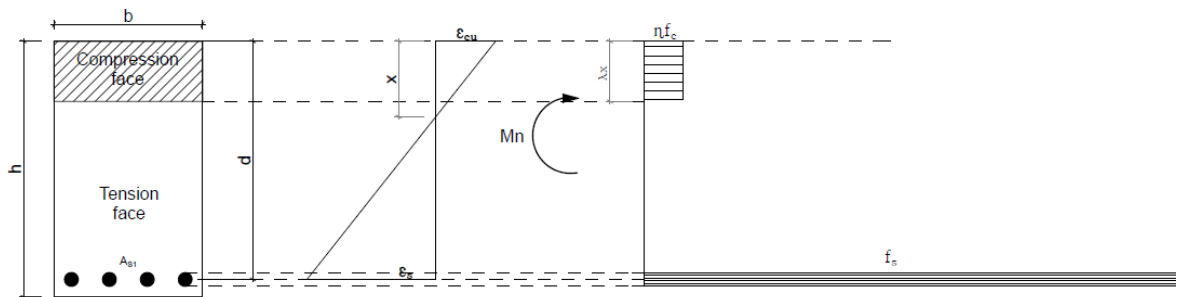


Figure 2.4.1 Singly RC Beam section with calculated strain and stress distributions

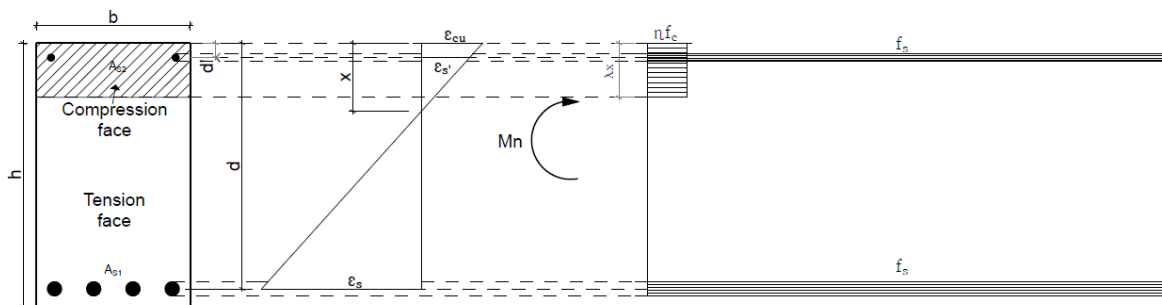


Figure 2.4.2 Doubly RC Beam section with calculated strain and stress distributions

In Figure 2.4.1 and Figure 2.4.2 it can be seen how the resulted strains and stresses are acting on the beam. When applying compression reinforced the bending moment is increasing, adding more strength to the structure, and the neutral axis , x , is decreasing in depth forcing the concrete contribution for compression to become smaller.

3 Numerical Analysis

In this chapter a finite element analysis is performed on an elastic perfectly-plastic reinforced concrete beam with particular failure criterion used in its plastic behaviour. The interest is concentrated in obtaining the moment- rotation curve and the distribution of the stresses and strains for the concrete material.

The process of modelling the reinforced beam is presented in this chapter. The analysis is carried out in the same manner for both singly and doubly reinforced concrete, therefore the steps leading to the final results are going to be presented just once.

3.1 Material Properties

The material behaviour for both concrete and steel is presented in this section along with the parameters used for the elastic state and the parameters inputted for the yield conditions adopted for the plasticity of the materials. Idealized elastic-perfectly plastic stress-strain behaviour is used for every analysis, this approach leads to the assumption that plastic yielding can occur only when the stress in the material reaches the value of the yielding stress and a perfectly straight yield plateau is formed with a constant stress and increasing strain until failure (5).

3.1.1 Concrete

The elastic behaviour of the concrete is modelled considering simple linear elasticity with Young modulus of elasticity and Poisson ratio as the material constants. Young modulus of elasticity represents a stiffness parameter and is defined as the ratios of the stress over strain. Poisson ratio is defined as the negative ratio of transversal rate of expansion of the strain over the axial contracting rate of strain when subjected to compression. The values for both parameters are presented in Table 3.1.1

Young's Modulus	$30 \times 10^3 \frac{\text{N}}{\text{mm}^2}$
Poisson ratio	0.2

Table 3.1.1 Elastic parameters for concrete

For the plastic state, where the deformations become irreversible, three constitutive models are adopted for the representation of the failure envelope. These failure criteria are defined as hypothesis since the nonlinear behaviour of concrete cannot provide exact solutions based on natural laws (7)

Mohr Coulomb failure criterion is a pressure-dependent model, highly used for brittle materials like concrete. It is based on the fact that the material becomes stronger as the pressure increases. From the theory explained in detail in Appendix C we know that:

$$k\sigma_1 - \sigma_3 - \sigma_c = 0 \quad (3.1.1)$$

$$f_c = 2c \times \sqrt{k} \quad (3.1.2)$$

$$k = \frac{1 + \sin\phi}{1 - \sin\phi} \quad (3.1.3)$$

Where:

k Material parameter

ϕ Angle of internal friction

c Cohesion

f_c Compressive strength of concrete

The angle of internal friction, ϕ , is a material parameter that defines the parameter k . The other parameter that is used by this yield criterion is the cohesion, c , which is determined by equation (3.1.4)

$$c = \frac{f_c}{2 \times \sqrt{k}} \quad (3.1.4)$$

In Figure 3.1.1 the shape of yield surface can be seen in the deviatoric plane which represents a plane that is perpendicular to the hydrostatic axis, an axis that is created on the principle stresses coordinate system when all the three principal stress are equal.

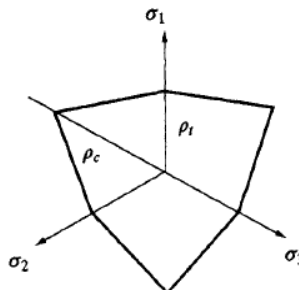


Figure 3.1.1 Mohr-Coulomb deviatoric plane (8)

Dilation angle is another parameter for Mohr-Coulomb analysis, it is assumed to be a constant and it controls deformation during plastic flow (9)

All the parameters required and their values for Mohr-Coulomb criterion are presented in Table 3.1.2 (8).

Angle of internal friction	37°
Dilation angle	31°
Cohesion	7.5 $\frac{\text{N}}{\text{mm}^2}$

Table 3.1.2 Mohr-Coulomb parameters

Concrete Damage Plasticity model represents an adaptation of the Druker-Prager criterion and it accounts for various evolution of strength under tension and compression (10). The adjustment made for this model is that the failure surface in the deviatoric plane is not necessarily a circle and its shape is given by a parameter K_c . As seen in Figure 3.1.2 the shape of the failure surface used in this analysis is the one when $K_c = \frac{2}{3}$, value recommended by Abaqus User's Manual (10).

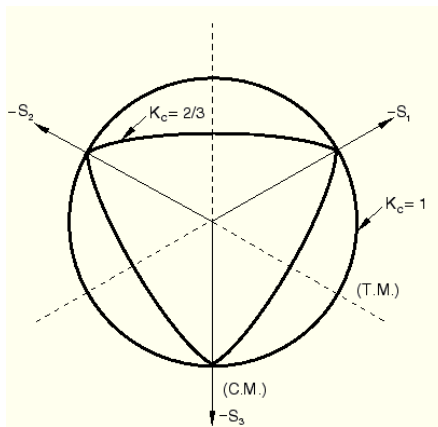


Figure 3.1.2 Concrete damage plasticity deviatoric plane (10)

Yield function:

$$F = \frac{1}{1-\alpha} (q - 3\alpha p + \beta(\varepsilon^{pl})(\sigma_{max}) - \gamma(-\sigma_{max})) - \sigma_c(\varepsilon_c^{pl}) = 0 \quad (3.1.5)$$

$$\alpha = \frac{\left(\frac{\sigma_{b0}}{\sigma_{c0}}\right) - 1}{2\left(\frac{\sigma_{b0}}{\sigma_{c0}}\right) - 1}; \quad 0 \leq \alpha \leq 0.5 \quad (3.1.6)$$

$$\beta = \frac{\sigma_c(\varepsilon_c^{pl})}{\sigma_t(\varepsilon_t^{pl})} (1 - \alpha) - (1 + \alpha) \quad (3.1.7)$$

$$\gamma = \frac{3(1 - K_c)}{2K_c - 1} \quad (3.1.8)$$

σ_{max} Maximum principal effective stress

$\frac{\sigma_{b0}}{\sigma_{c0}}$ Ratio of initial equibiaxial compressive yield stress to initial uniaxial compressive yield stress

K_c Ratio of the second stress invariant on tensile meridian, $q(TM)$, to that on the compressive meridian, $q(CM)$

$\sigma_t(\varepsilon_t^{pl})$ Effective tensile cohesion stress

$\sigma_c(\varepsilon_c^{pl})$ Effective compressive cohesion stress

The value for dilation angle is taken to be identical as in the Mohr-Coulomb plasticity and the recommended values by Abaqus are used for the other parameters needed. Their values are presented in Table 3.1.3.

Dilation angle	31°
Flow potential eccentricity	0.1
Biaxial/Uniaxial compression plastic strain ratio	1.16
Invariant stress ratio K_c	0.6667
Viscosity	0
Compression yield stress	30 $\frac{\text{N}}{\text{mm}^2}$
Inelastic strain	0
Tensile yield stress	3 $\frac{\text{N}}{\text{mm}^2}$
Tensile cracking strain	0

Table 3.1.3 Concrete damage plasticity parameters

3.1.2 Steel

For the analysis of steel the parameters are presented in Table 3.1.4

Young's Modulus	$2 \times 10^5 \frac{\text{N}}{\text{mm}^2}$
Poisson ratio	0.3
Yield stress	$460 \frac{\text{N}}{\text{mm}^2}$
Plastic strain	0

Table 3.1.4 Elastic and plastic parameters for concrete

3.2 Geometry

The geometry is realized considering the geometry parameters presented in Table 1.1.1 and two models are formed on the same principles as in the analytical analysis, one just with tensile reinforcement and the second model with both tensile and compression reinforcement. The concrete part of the geometry and the reinforcement part are done separately as 3D deformable solid elements and merged together in the assembly module with the use of parallel face constrain, to align the reinforcement on the same direction with the concrete beam, and translating instances, to place the reinforcements on the corresponding location. It is important to specify that the concrete is chosen to be suppressed by the corresponding steel reinforcement.

In order to get the stress and strains at the end of the analysis a partition is defined on the full geometry beam at its middle length, $\frac{L}{2}$, and a number of 33 points are created in a line that passes through the centre of the beam section and is perpendicular to the x-z plane, as displayed in Figure 3.2.1

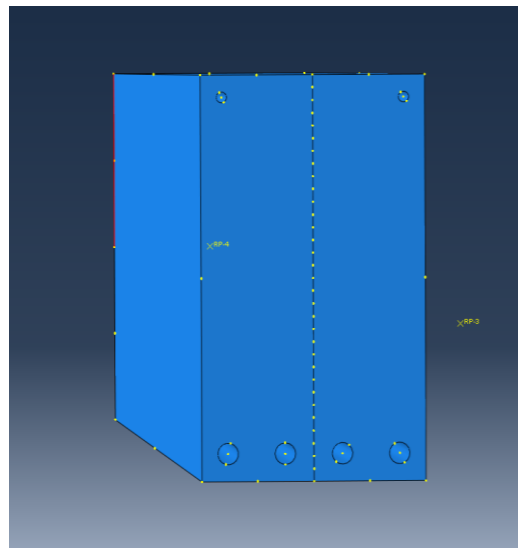


Figure 3.2.1 Middle section of doubly RC Beam model

Finally the full beam geometry is presented in Figure 3.2.2

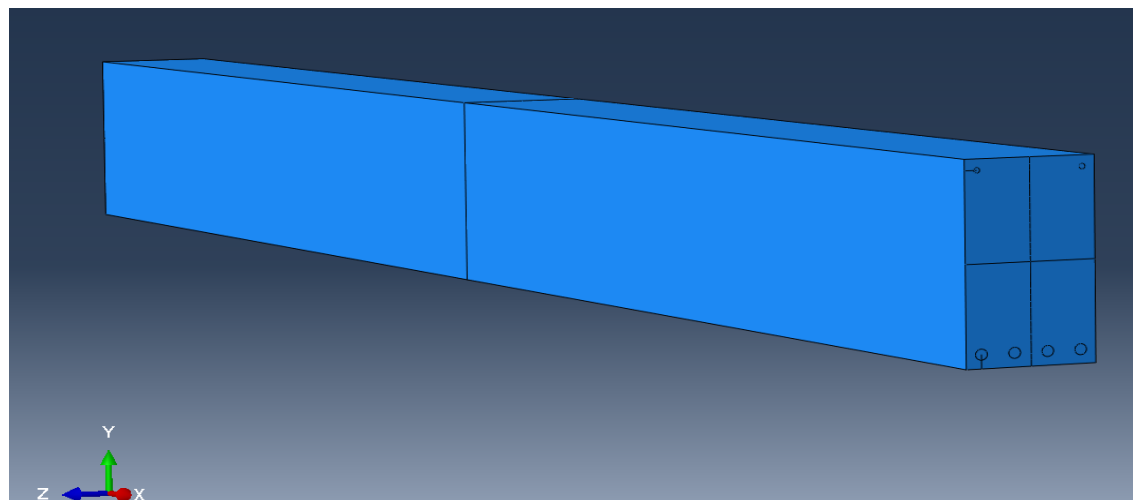


Figure 3.2.2 Doubly RC Beam

3.3 Boundary Conditions and Constraints

The boundary conditions and the types of constraints applied on the geometry presented in section 3.2 in order to model the beam in Abaqus in the same way as the static system from the analytical part presented in Figure 2.1.1. is shown in this part

Firstly, two reference points are assigned on the middle of each end of the beam's faces, and rigid body constrains are applied over the end surface to the corresponding reference point, so in that way both end surfaces of the beam are controlled from the reference points.

The boundary conditions are defined in Abaqus as in Figure 3.3.1

- 1 Translation in the 1-direction (U1).
- 2 Translation in the 2-direction (U2).
- 3 Translation in the 3-direction (U3).
- 4 Rotation about the 1-direction (UR1).
- 5 Rotation about the 2-direction (UR2).
- 6 Rotation about the 3-direction (UR3).

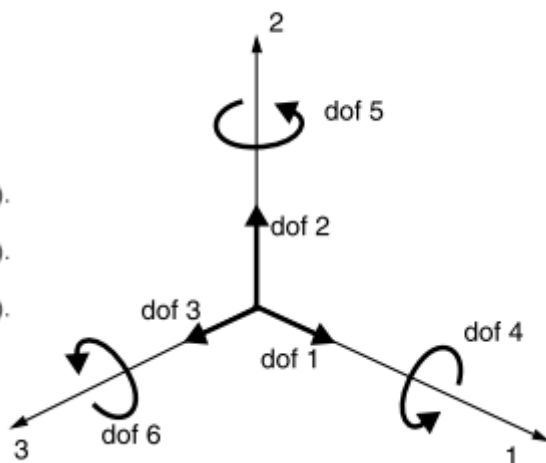


Figure 3.3.1 Boundary Conditions notation in Abaqus (10)

In this particular case the directions 1, 2 and 3 represent the x, y and z axis.

For a the reader to have a better understanding on how the boundary condition are applied a 2D sketch of the beam is made as displayed in Figure 3.3.2.

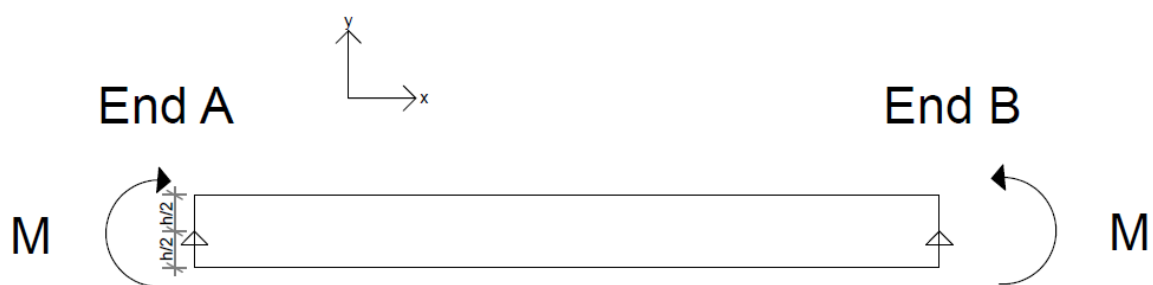


Figure 3.3.2 RC Beam sketch

In order to model the supports the following boundary conditions are assigned in the reference point from end A:

$$U1 = 0$$

$$U2 = 0$$

$$U3 = 0$$

$$UR1 = 0$$

BC in the reference point from end B:

$$U2 = 0$$

$$U3 = 0$$

The moments are applied through rotation boundary conditions also in the reference points therefore when they are acting on the structure they are generating deformations in the same manner as in the analytical part where the top section of the beam is acting on compression and the bottom section of the beam is subjected to tension.

The rotation BC are applied as follows:

At end A:

$$UR3 = -0.08 \text{ rad}$$

At end B

$$UR3 = 0.08 \text{ rad}$$

The rotation 0.08 radian it is a random value that is chosen after test analysis are performed and the results showed that the reinforced beam reaches the ultimate moment within this range 0- 0.08 radians.

The beam end surface is shown in Figure 3.3.3 with

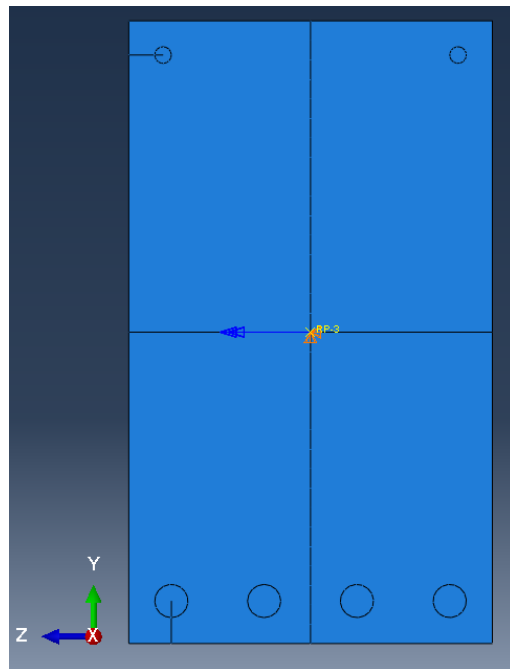


Figure 3.3.3 Middle section of doubly RC Beam model

3.4 Mesh system

One very important characteristic of Finite Element analysis is that the regions are divided into small part, so called finite elements, and the software calculates a solution over each individual element. The first step in meshing the model is choosing the right type of element and as it can be seen in Figure 3.4.1 there are several types of element available in Abaqus for three dimensional analyses. However due to the round geometry inside the model created by the reinforcement and as the software states in the mesh module that the RC beam is unmeshable with hexes or wedges, the tetrahedral quadratic element is used in this project.

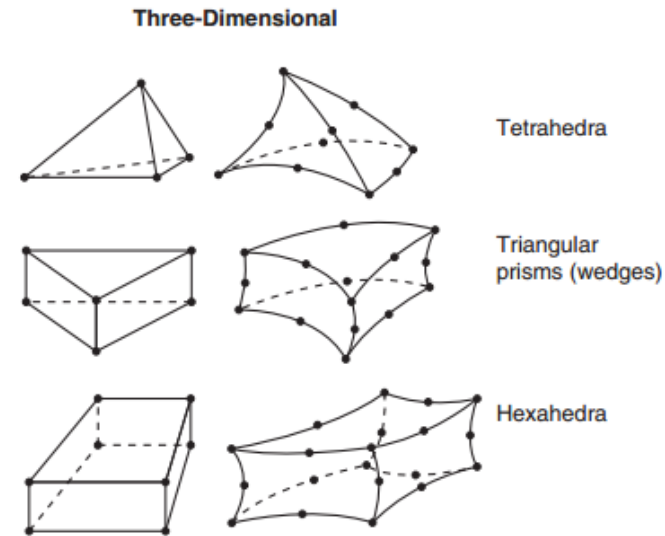


Figure 3.4.1 Middle section of doubly RC Beam model

In order to validate the comparison between the test that are performed, a crude converge analysis is done at the start of the project and it is seen that the mesh is not very flexible with the number of elements on the model, since there are multiple nodes created inside the RC beam and each node from the geometry corresponds to a node in the mesh element. However it is concluded that finite element results do not vary more than 5% and a compromise is made between the density of the elements in the mesh and the computational time. Further, the same parameters used to generate the mesh from the first analysis performed, which was a singly RC beam with concrete damage plasticity, are used on all the test completed all along the project.

In Figure 3.4.2 the mesh can be visualized.

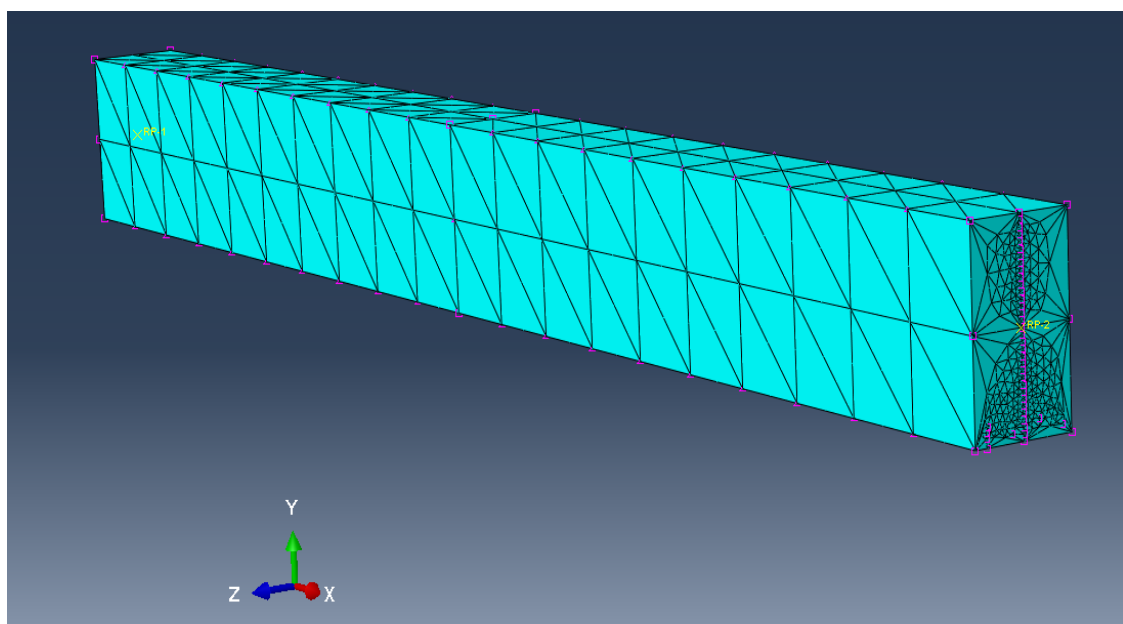


Figure 3.4.2 Mesh system with tet elements

3.5 Results

After all the analysis steps are performed the corresponding result that are in this project interest are taken from Abaqus software and plotted for further interpretation as follows. The bending moment of the structure is taken from one of the reference points and plotted over the rotation that is applied to the beam.

For stresses and strains, firstly a view cut is activated on the beam to view the points that are created on the middle length of the beam, shown in Figure 3.2.1, and a node path is set up. Along this node path the stresses and the strains are visualised.

The results are presented bellow for singly RC beam and for doubly RC beam.

3.5.1 Singly RC beam

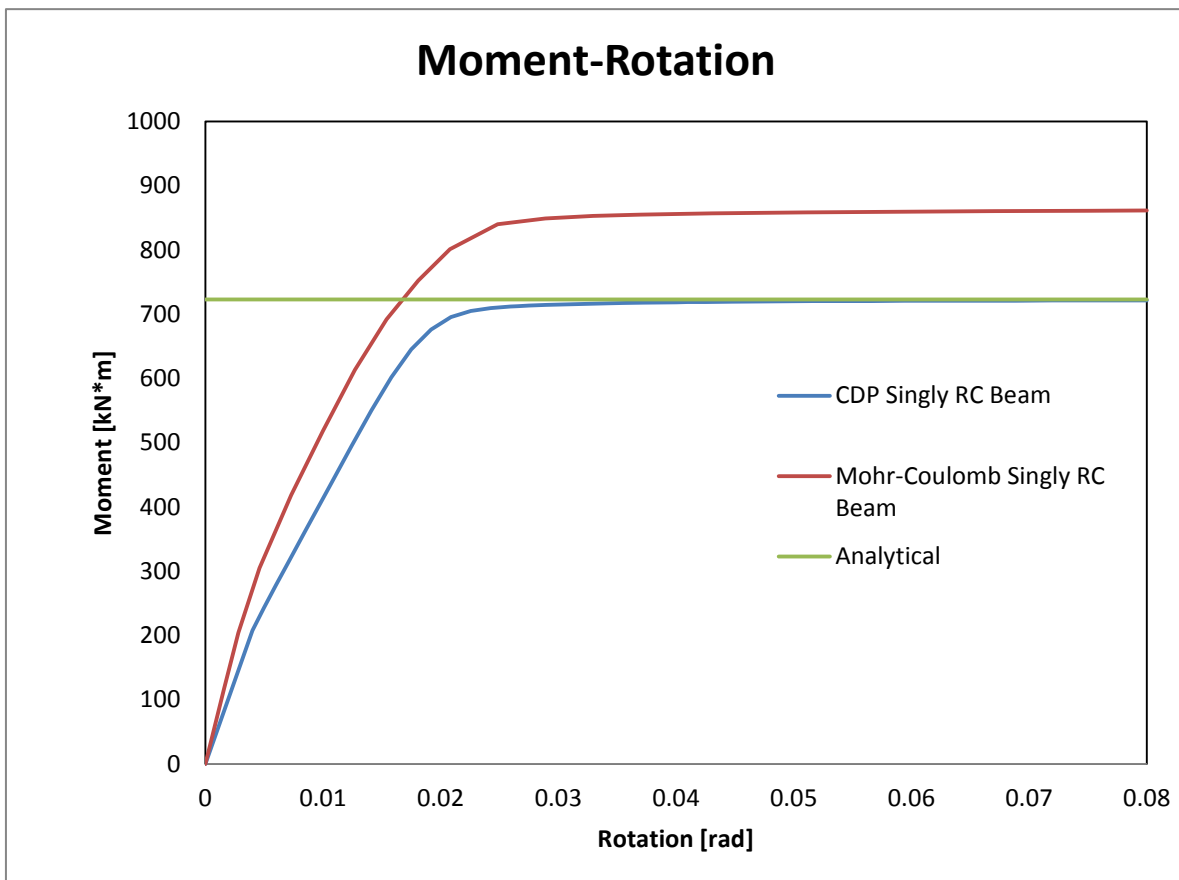


Figure 3.5.1 Moment-Rotation relation

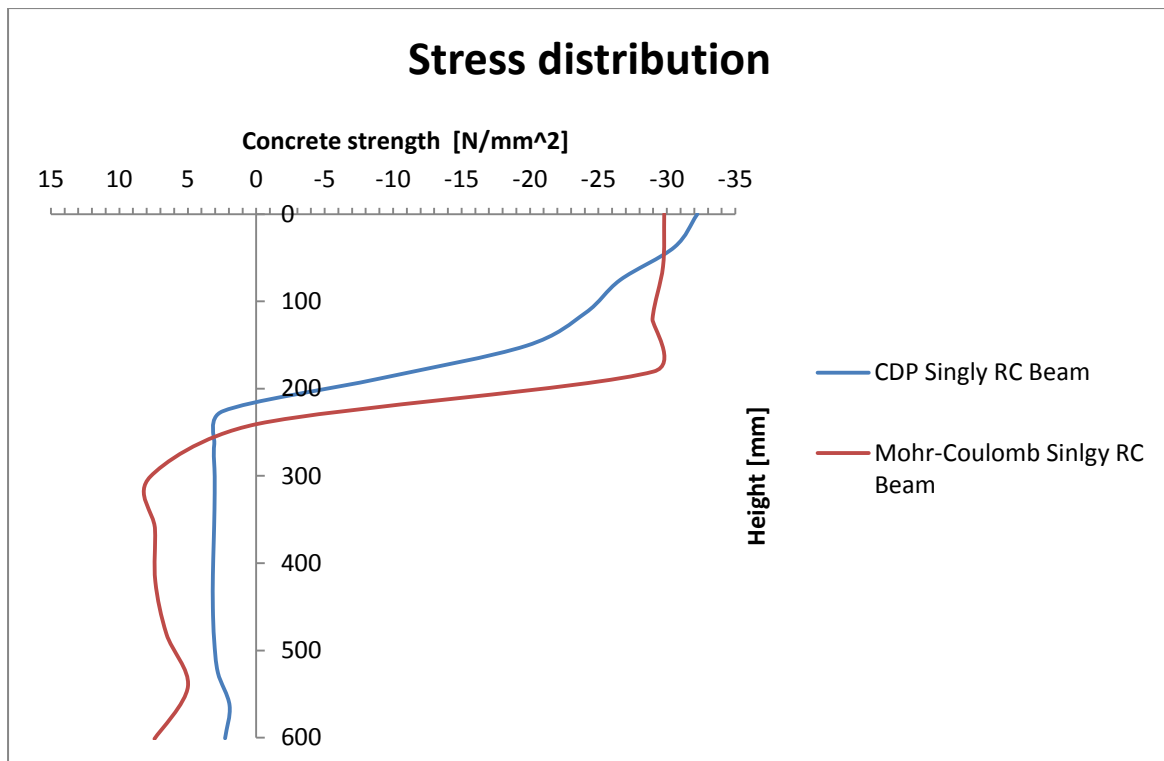


Figure 3.5.2 Stress distribution

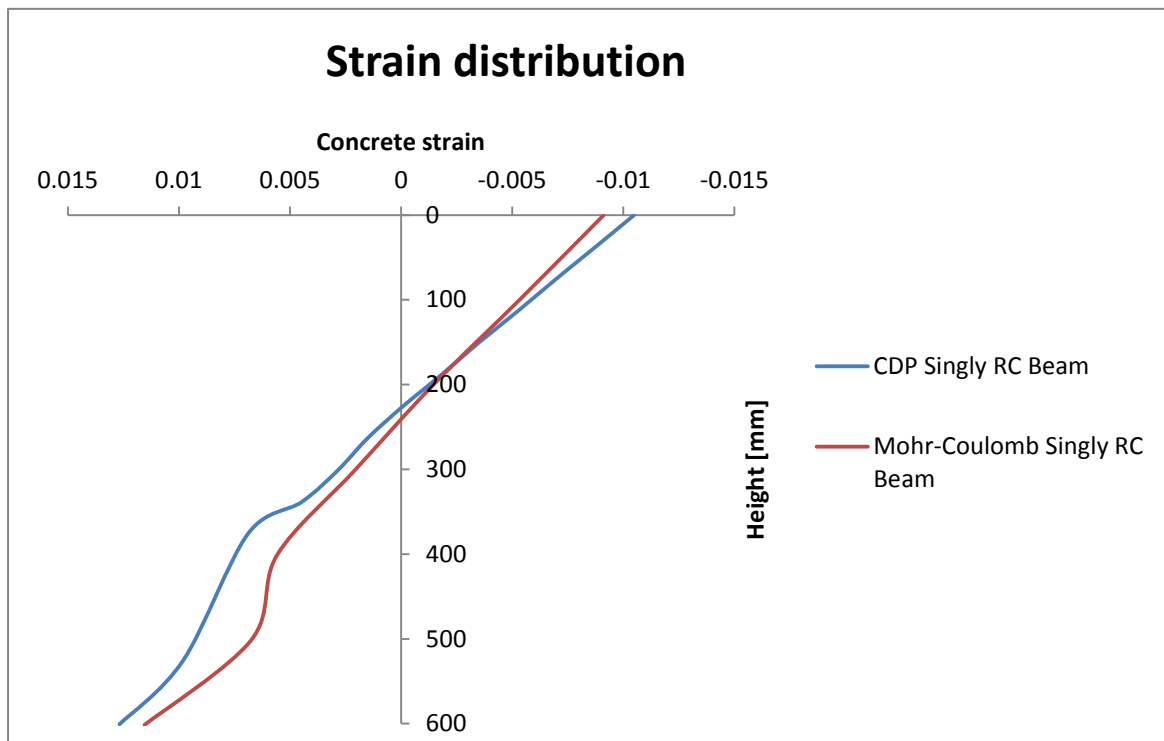


Figure 3.5.3 Strain distribution

3.5.2 Doubly RC beam

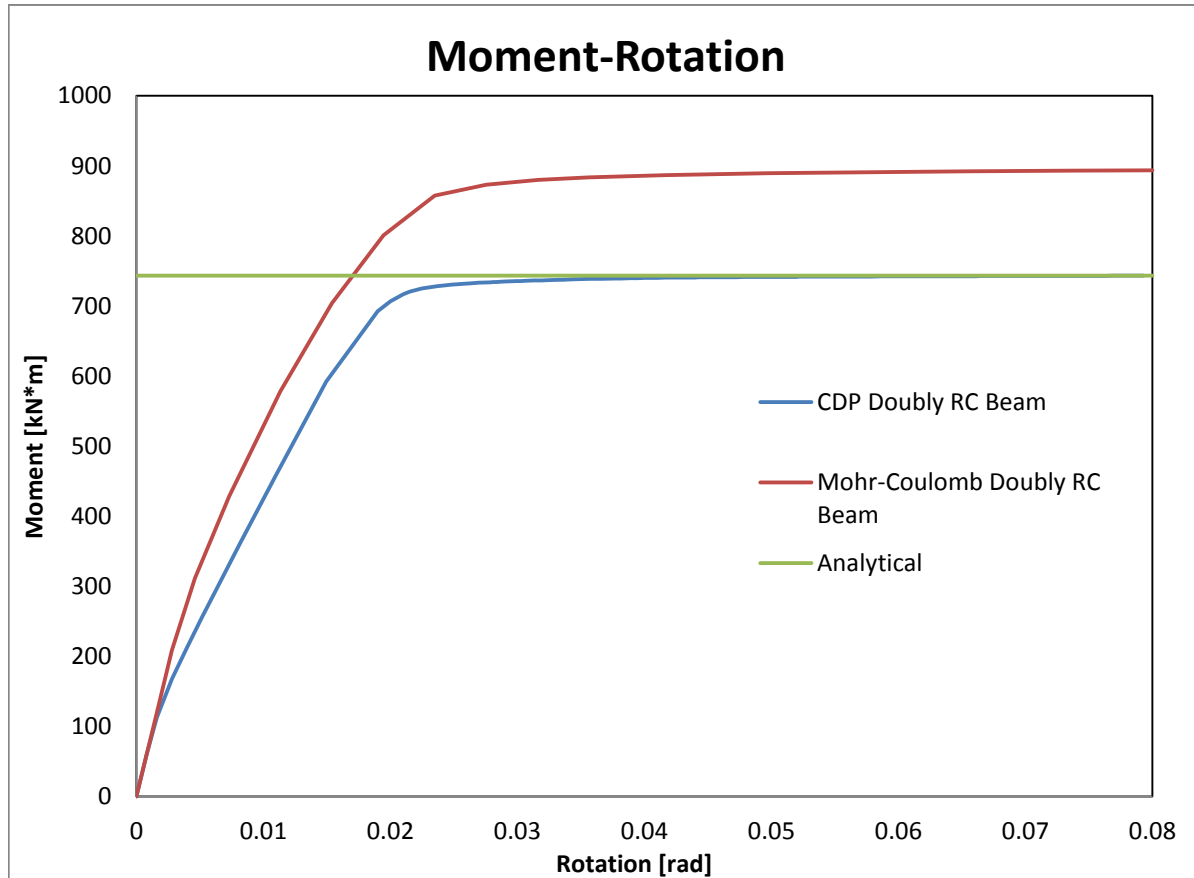


Figure 3.5.4 Moment-Rotation relation

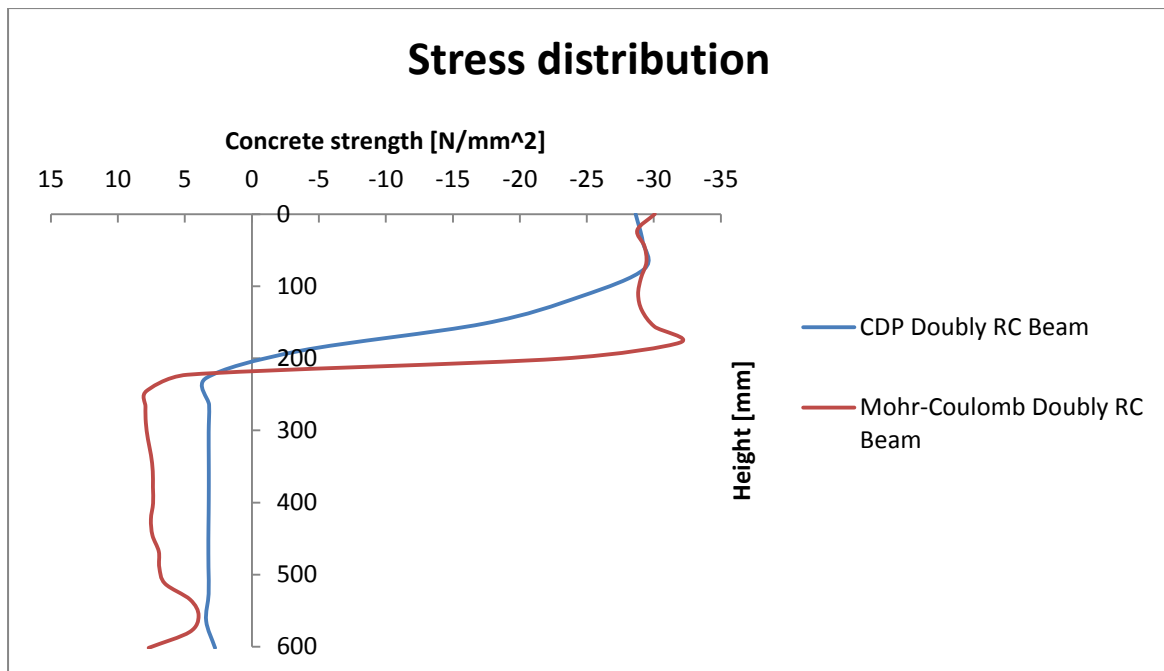


Figure 3.5.5 Stress distribution

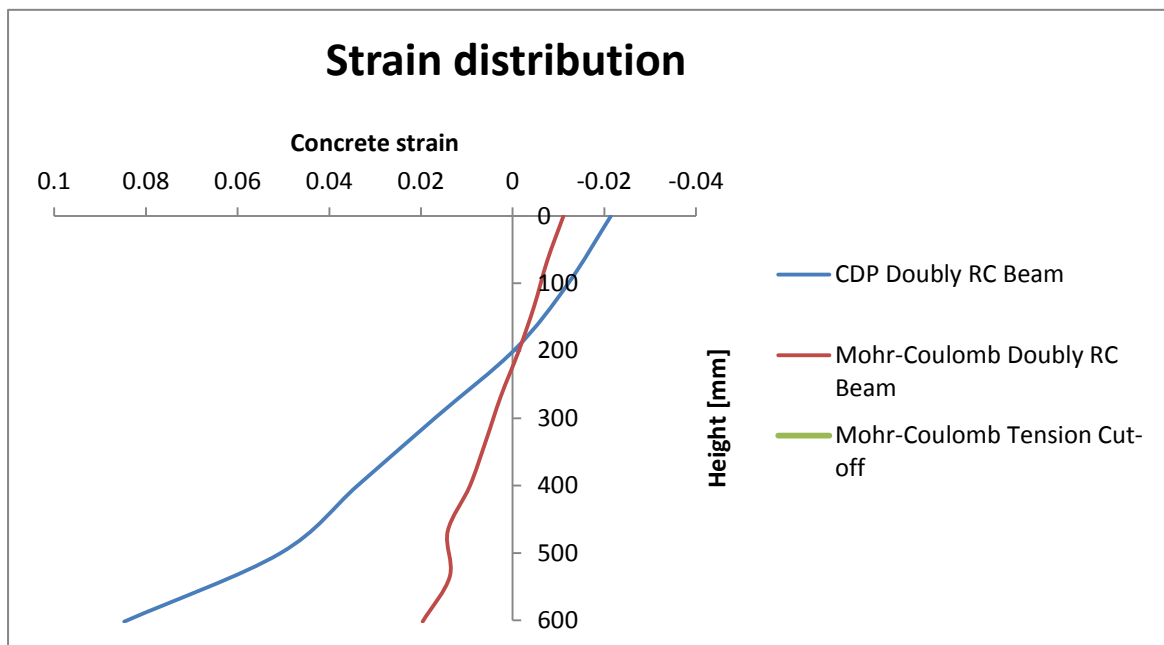


Figure 3.5.6 Strain distribution

3.5.3 Conclusion of the result

Regarding the result displayed above it appears that Mohr-Coulomb overestimates the tensile strength of concrete in the same manner as stated in (8) where it is mentioned that Mohr-Coulomb predicts a value of about 25% of the strength of concrete in compression which is far too large than the actual tensile strength of concrete. This can explain why the moment capacity is higher than the one from concrete damage plasticity. As a solution to this issue a tension cut off can be applied to the Mohr-Coulomb analysis, however it seems that the Mohr-Coulomb in Abaqus is not highly stable and when tension cut-off is applied to the model it doesn't converge to a solution.

Concrete Damage Plasticity appears to be more stable and to provide more accurate result, for this reason the results from this analysis are going to be compared further with the analytical result in Chapter 4

4 Comparison

A comparison between Concrete Damage plasticity model and analytical analysis is done in this chapter following a discussion and the final conclusion in the last chapter.

4.1 Bending moment

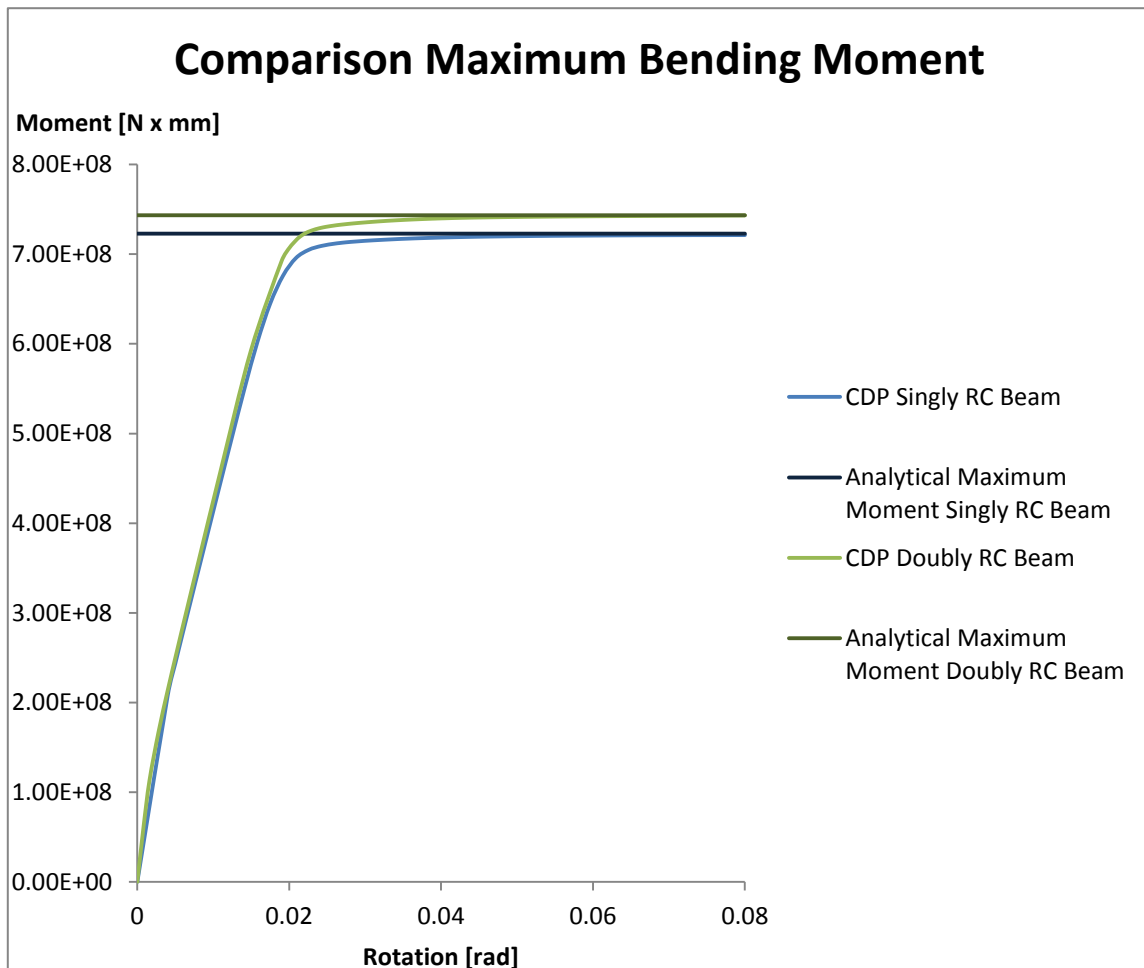


Figure 4.1.1 Moment-Rotation relation

The results from Concrete Damage plasticity and the Analytical ones appear to fit perfectly, however it is important to mention that with a denser mesh the moments obtained in Abaqus tend to have a slight increase, but due to the long computational hours it was decided that the minor changes are not bringing any benefits.

4.2 Stresses

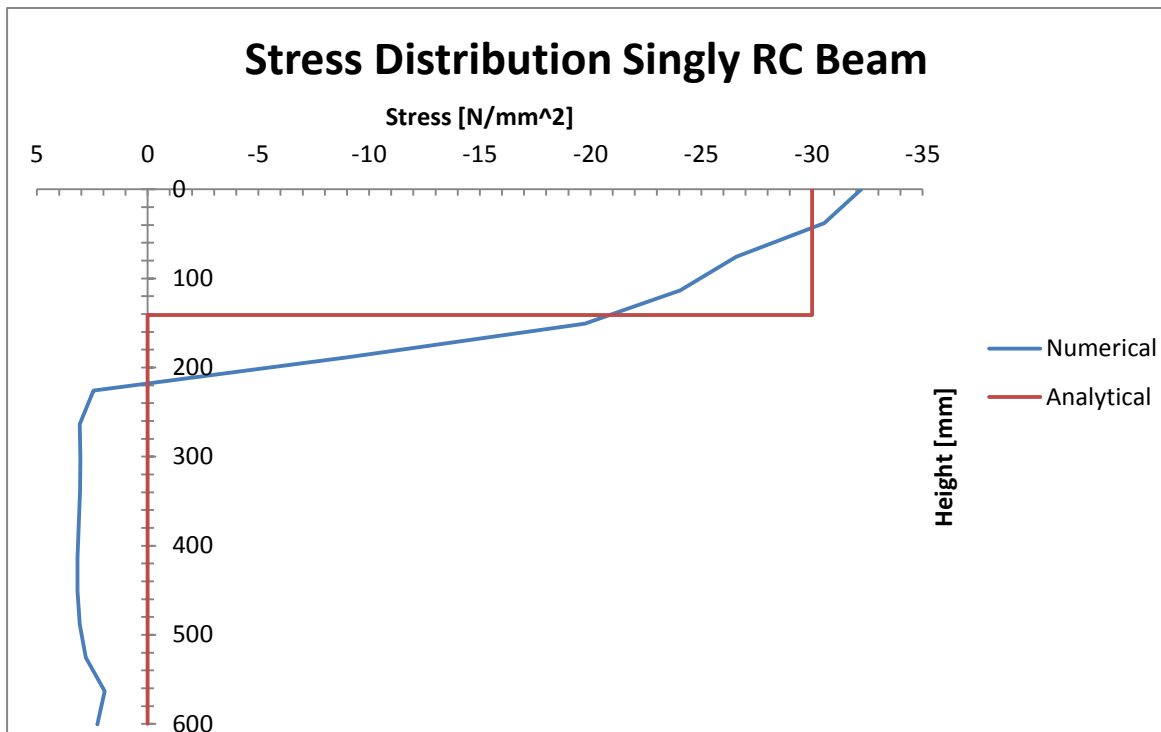


Figure 4.2.1 Stress distribution

Stress Distribution Doubly RC Beam

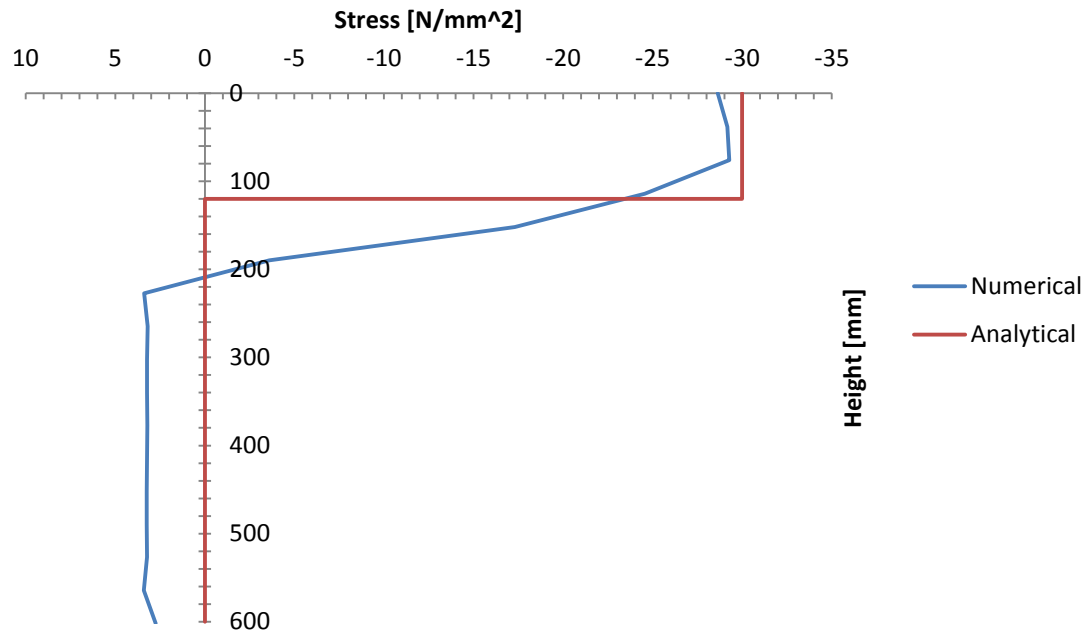


Figure 4.2.2 Stress distribution

4.3 Strains

Strain Distribution Singly RC Beam

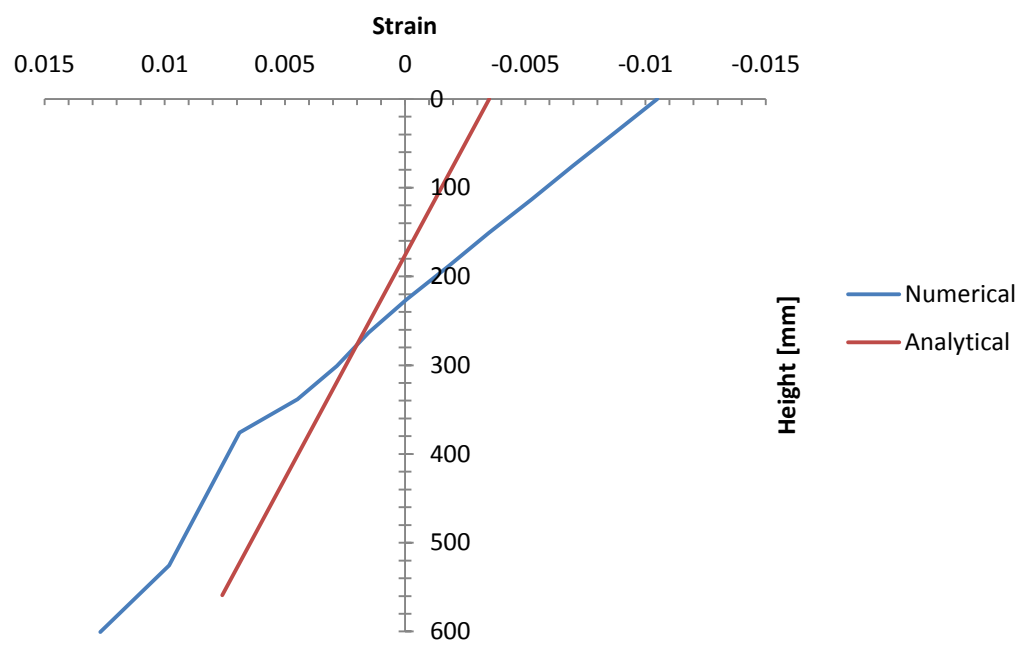


Figure 4.3.1 Strain distribution

Strain Distribution Doubly RC Beam

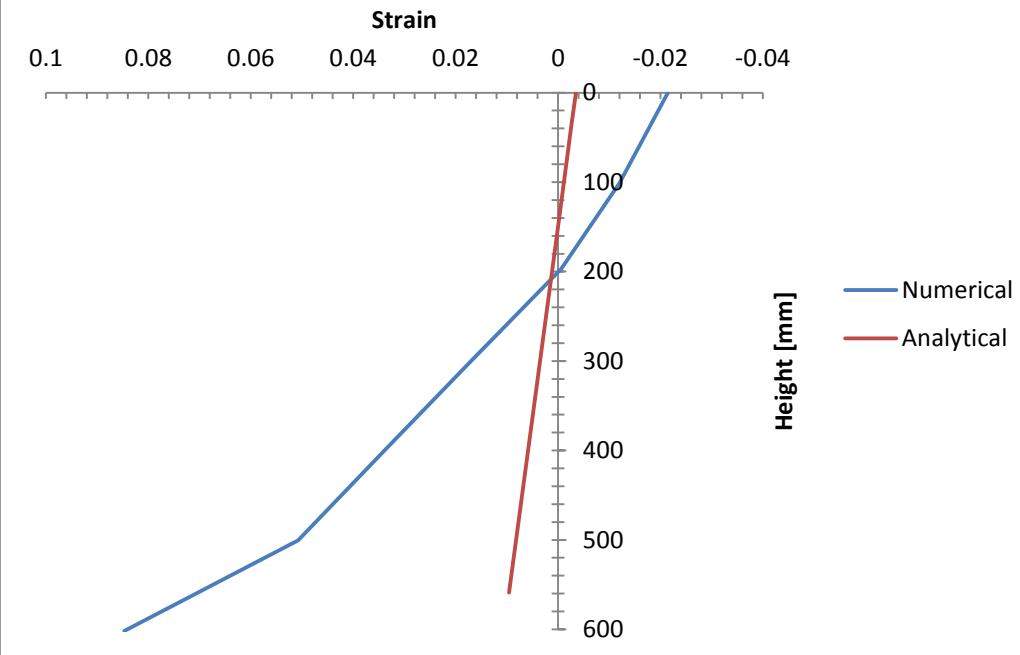


Figure 4.3.2 Strain distribution

5 Conclusion

This master thesis has as an objective to identify the advantages and disadvantages of performing a Finite Element analysis on reinforced concrete beams modelled as an elastic perfectly-plastic material with different failure hypothesis.

The numerical bending moment capacity obtained from concrete damage plasticity is found to be in close agreement with the analytical maximum bending capacity giving almost the same results. Regarding the stresses, it also gives accurate predictions as it is known that the stress block of concrete used in analytical calculations is a simplification to the real stress distribution demonstrated by experiments. The strains turn out to be higher than the strains obtained from analytical result which can be due to the fact that the assumptions from Eurocode for the ultimate concrete strain are so conservative for safety reasons.

The Mohr-Coulomb criterion from Abaqus appears to be unpredictable, requiring a higher complexity level in constructing the model, it could be because in Abaqus associated plasticity, when friction angle is equal to the dilation angle is impossible to apply, as a result non-associated plasticity is used which causes a lot of computational problems. For this reason a Mohr-Coulomb analysis with tension cut-off that would correct the initial overestimation of simple Mohr-Coulomb regarding the tensile strength of concrete.

The constitutive model concrete smeared cracking is also attempted in this project however the results are inconclusive as the analysis cannot converge as an elastic-perfectly plastic material; it requires tension stiffening parameters to define the post-failure behaviour of concrete.

As a final conclusion it can be stated that reinforced concrete material is a non-homogenous material with a complex behaviour that requires a high level of consideration when its plastic behaviour is analysed. This particular study concludes that concrete damage plasticity model is highly suitable for providing accurate result on elastic perfectly plastic behaviour of reinforced concrete.

Bibliography

1. **M. Nadim Hassoun, A. Al-Manaseer.** *Structural Concrete Theory and Design* . New Jersey : John Wiley & Sons, 2005.
2. *EN 1992-1-1 (2004): Eurocode 2: Design of concrete structures.*
3. **D.W.Kirk, S.U.Pillai and.** *Reinfocred concrete design* . 1988.
4. **Nawy, Edward G.** *Reinforced Concrete - A fundamental approach*. New Jersey : s.n., 2000.
5. **Milan Jirasek, Zdenek P. Bazant.** *Inelastic Analysis of Structures*. 2002.
6. **Moy, Stuart S. J.** *Plastic Methods for Steel and Concrete Structures*. 1996.
7. **M.P.Nielsen.** *Limit Analysis and Concrete Plasticity*. s.l. : CRC Press, 1999.
8. **Niels Saabye Ottosen, Matti Ristinmaa.** *The Mechanics of Constitutive Modelling*. 2005.
9. **Bartlett, Steven F.** Mohr-Coulomb Model. *civil.utah.edu*. [Online] 2012.
10. **Dassault Systèmes.** *Abaqus Analysis User's Manual*. 2013.
11. **McCormac, Jack C.** *Design of Reinforced Concrete*. s.l. : John Wiley & sons, 2001.